

See discussions, stats, and author profiles for this publication at: <https://www.researchgate.net/publication/281457031>

End Capping Does Matter: Enhanced Order and Charge Transport in Conjugated Donor–Acceptor Polymers

ARTICLE *in* MACROMOLECULES · SEPTEMBER 2015

Impact Factor: 5.8 · DOI: 10.1021/acs.macromol.5b01252

READS

56

9 AUTHORS, INCLUDING:

[Sreenivasa Reddy Puniredd](#)

Agency for Science, Technology and Research ...



48 PUBLICATIONS 770 CITATIONS

[SEE PROFILE](#)

[George D. Kamenov](#)

University of Florida

138 PUBLICATIONS 1,606 CITATIONS

[SEE PROFILE](#)



[Wojciech Pisula](#)

Max Planck Institute for Polymer Research

213 PUBLICATIONS 9,024 CITATIONS

[SEE PROFILE](#)

End Capping Does Matter: Enhanced Order and Charge Transport in Conjugated Donor–Acceptor Polymers

Unsal Koldemir,[†] Sreenivasa Reddy Puniredd,^{§,¶} Manfred Wagner,[§] Sefaattin Tongay,[⊥] Tracy D. McCarley,[#] George Dimitrov Kamenov,[‡] Klaus Müllen,^{*,§} Wojciech Pisula,^{*,§,%} and John R. Reynolds^{*,||}

[†]The George and Josephine Butler Polymer Research Laboratory, Department of Chemistry, Center for Macromolecular Science and Engineering, and [‡]Department of Geology, University of Florida, Gainesville, Florida 32611, United States

[§]Max Planck Institute for Polymer Research, Ackermannweg 10, 55128 Mainz, Germany

[#]Institute of Materials Research and Engineering, A*STAR (Agency for Science, Technology and Research), 3 Research Link, 117602 Singapore

[¶]School of Chemistry and Biochemistry, School of Materials Science and Engineering, Center for Organic Photonics and Electronics, Georgia Institute of Technology, 901 Atlantic Drive, Atlanta, Georgia 30332, United States

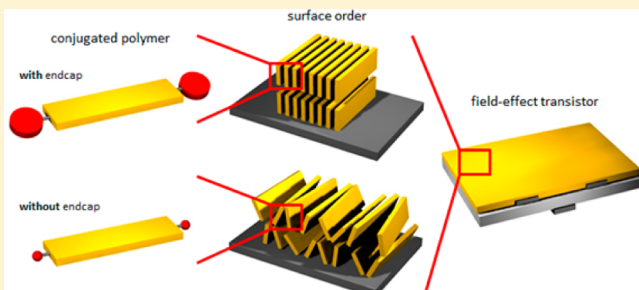
[⊥]Materials Science and Engineering, School for Engineering of Matter, Transport and Energy, Arizona State University, Tempe, Arizona 85287, United States

^{*}Department of Chemistry, Louisiana State University, Baton Rouge, Louisiana 70803, United States

^{||}Department of Molecular Physics, Faculty of Chemistry, Lodz University of Technology, 90-924 Lodz, Poland

Supporting Information

ABSTRACT: Optimized microstructure through control of both intra- and intermolecular interactions in organic semiconductors is critical for enhancing and optimizing charge transport for the realization of next-generation low-cost, mechanically flexible, and easy to process high performance, organic field effect transistors (OFETs). Herein, we report donor–acceptor alternating copolymers of dithienogermole (DTG) with 2,1,3-benzothiadiazole (BTD) and probe the importance of end groups on the control of molecular order and microstructure as it relates to the enhancement of charge carrier transport. Partial end-capping reactions, confirmed by ¹H NMR and matrix-assisted laser desorption/ionization mass spectrometry (MALDI-MS) analyses, on the DTG–BTD copolymer provided significant improvement in grazing incidence wide angle X-Ray scattering (GIWAXS) determined polymer ordering in thin films. Consequently, OFETs exhibited charge-carrier mobilities up to 0.60 cm²/(Vs) for the end-capped copolymer, which are an order of magnitude higher in comparison to the non-end-capped analogue, which displayed a mobility of 0.077 cm²/(Vs). We emphasize that a simple synthetic approach, the introduction of end-capping groups which remove reactive functionalities, can be effective in the development of next-generation OFET and solar materials by promising better control of the polymer organization.



INTRODUCTION

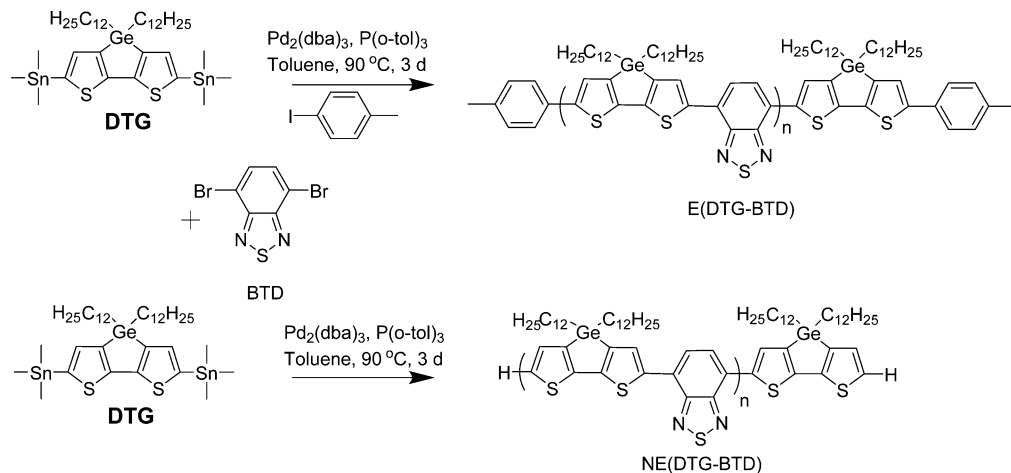
Solution deposited organic semiconductors with high charge carrier mobilities are required for the development of high performance organic field effect transistors (OFETs), which have potential utility in flexible and transparent displays. As conjugated polymers can be processed from solution, devices can be fabricated by inkjet printing or roll-to-roll processing techniques at ambient temperatures and pressures. These techniques give promise for mechanically flexible and durable, large area organic electronics, minimizing cost through eliminating the need for high vacuum environments. To date, solution processed conjugated polymers such as regioregular poly(3-hexylthiophene) (P3HT),^{1,2} poly(2,5-bis(3-alkylthio-

phen-2-yl)thieno(3,2-*b*)thiophene) (PBTTT) derivatives,^{3,4} and various donor–acceptor (D–A) polymers^{5–14} have been implemented in OFETs that yield charge carrier mobilities often exceeding 0.1 cm²/(Vs) and reaching as high as 10 cm²/(Vs).^{15,16}

Charge carrier transport in a polymeric organic semiconductor depends on a range of factors, which include repeat unit structure, along with order and crystallinity which is regulated by processing conditions. Of these, order and crystallinity in the

Received: June 16, 2015

Revised: August 10, 2015

Scheme 1. Chemical Synthesis and Repeat Unit Compositions for E(DTG–BTD) and NE(DTG–BTD)

solid state are especially crucial issues since structural defects can act as traps for charges and reduce device performance.¹⁷ In D–A polymers, the attainable order is influenced dramatically by the repeat unit structure and the positioning of the solubilizing alkyl chains, which control intrachain conjugation and interactions between the conjugated backbones.¹⁸ Strong or well-balanced intermolecular forces can reduce the π -stacking distance between polymer chains as they array into lamellar superstructures. A small π -stacking distance, resulting in short-range intermolecular aggregation, is the main cause for efficient long-range charge transport.^{19–23} In the context of controlling polymer order, a variety of parameters, such as the length/shape and substitution position of alkyl side chains,^{24–28} regioregularity,^{29,30} molecular weight,^{31–34} and backbone curvature,^{35–38} play important roles. For good film formation and adaptation of an adequate microstructure, a fine balance between attractive and repulsive forces can be tuned via these approaches. As the order within the organic semiconductor is also controlled by processing conditions, which includes temperature, concentration, solvent, evaporation rate, and surface modification, attaining optimized systems can be a complicated and material specific process. An effective processing technique such as dip-coating or solution-shearing can induce polymer alignment in the preferred direction, which significantly enhances the charge transport.¹⁹

Considering the role defects play in donor–acceptor copolymer structures, the impact that end groups have on molecular order and charge transport has been minimally probed to date. During the preparation of this manuscript, a few reports were published showing the enhancement of molecular packing for donor–acceptor polymers.^{39,40} In contrast, extensive research has been devoted to prepare end-functionalized P3HT, prepared via the chain growth type Grignard metathesis (GRIM) polymerization method, due to the chain-end reactivity.^{41–44} A variety of functional groups—phenyl, benzyl, vinyl, and allyl—have been incorporated as end groups and their incorporation confirmed by MALDI-MS and ^1H NMR techniques.^{45–52} To a more limited extent, end-capping reactions on conjugated polymers obtained via popular metal-mediated step-growth type polycondensations, such as the Kosugi–Migita–Stille, Suzuki–Miyaura, and the newly emerging direct arylation polymerization (DArP), have been used.^{7,53–59} The most common end-capping method involves reacting the difunctional monomers in a stoichiometric balance, followed by adding monofunctional end-cappers after the polymerization

is complete. However, the presence and characterization of the end groups have been overlooked due to the complexity of the conventional step-growth polymerizations, Kosugi–Migita–Stille and Suzuki–Miyaura, as they can undergo dehalogenation or demetalation reactions during the polymerizations.^{60,61} Postpolymerization end-capping reactions on donor–acceptor copolymers to create functional end groups that can undergo further cross-linking reactions have been reported. For instance, a fluorene–benzothiadiazole copolymer was postfunctionalized with vinyl moieties which were subjected to cross-linking to tune the photoemission.⁶² Alternatively, an *in situ* end-capping protocol was introduced in which a three-component Kosugi–Migita–Stille polycondensation was employed with a difunctional diketopyrrolopyrrole and thiophene and a monofunctional perylene diimide as the end-capping unit.⁶³

In order to probe the effect of end-capping on the structural and electronic properties of a D–A conjugated polymer, we have synthesized end-capped alternating copolymers of dithienogermeole (DTG) with 2,1,3-benzothiadiazole (BTD) to yield a DTG–BTD copolymer and compared its properties to a non-end-capped analogue. The end-capped DTG–BTD copolymer was synthesized via Kosugi–Migita–Stille polycondensation by reacting a 1% excess of the distannylated DTG with a dibrominated BTD unit, followed by postfunctionalization with 4-iodotoluene. This was carried out with the *a priori* assumption that the chains were all stannyl terminated based on the stoichiometric imbalance used during the polymerization. As will be discussed later in relation to the MALDI-MS results, this is not the case, and the exact identity of the chain ends is complex. We did a broad examination of the nature of end groups with ^1H NMR and MALDI-MS and elaborated on the reason for batch-to-batch variability resulting in conjugated polymers due to the extent of polymerization reaching below unity in these kinds of complex polycondensations. End-capping protocol with stoichiometric imbalance has been employed in the preparation of *high band gap* phthalocyanine end-functionalized benzodithiophene-based copolymers and norbornene end-functionalized fluorene copolymers.^{64,65} Additionally, by varying the ratio of difunctional AA/BB monomers have been pursued for generating controlled molecular weight low and medium band gap conjugated polymers using the Carothers equation.^{40,66} In our work, the DTG–BTD system has been chosen for its enhanced attractive π – π interactions between polymer chains due to the longer C–Ge bond lengths in the fused thiophene ring

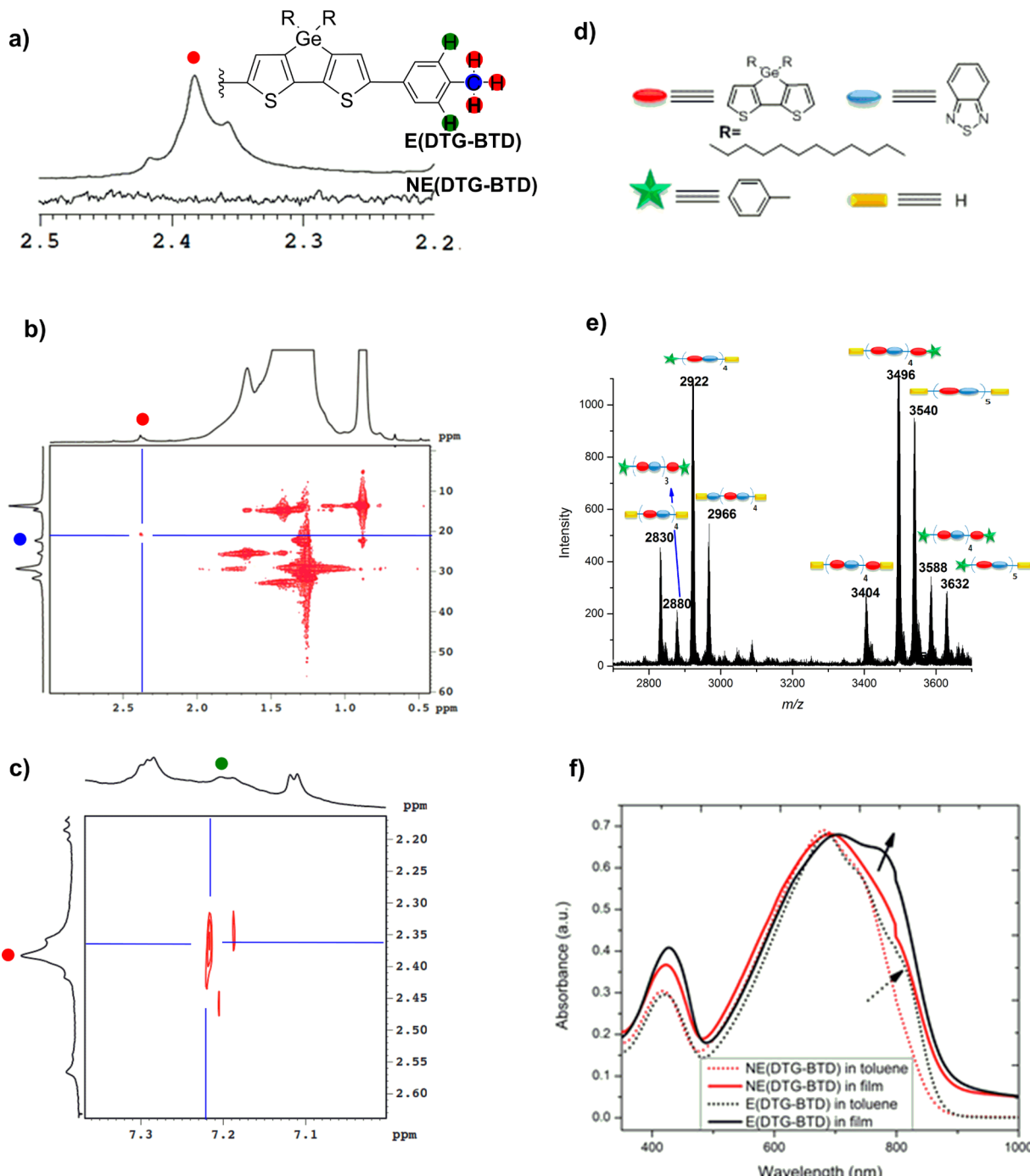


Figure 1. (a) ^1H NMR (500 MHz) of E(DTG–BTD) and NE(DTG–BTD) at 373 K in $\text{C}_2\text{D}_2\text{Cl}_4$ between 2.2 and 2.5 ppm. (b) ^1H – ^{13}C 2D HSQC (^1H (500 MHz), ^{13}C (125 MHz)) of E(DTG–BTD) at 373 K in $\text{C}_2\text{D}_2\text{Cl}_4$. (c) ^1H , ^1H 2D NOESY (500 MHz) of E(DTG–BTD) at 373 K in $\text{C}_2\text{D}_2\text{Cl}_4$. (d) Representative cartoon shapes for the oligomer residues for the MALDI mass spectrum of E(DTG–BTD). (e) MALDI mass spectrum of E(DTG–BTD) in the expanded region of m/z 2700–3700. (f) Absorption spectra for dilute solutions of E(DTG–BTD) and NE(DTG–BTD) in toluene and for thin film. Arrows highlight the aggregation bands.

which move *n*-dodecyl solubilizing side chains away from the polymer backbone.⁶⁷ Tolyl moieties were chosen as end groups, similar to previous reports on P3HT, as they play a minimal role in the polymer's electronic properties while yielding facile characterization by ^1H NMR due to their characteristic chemical shift that does not overlap with the resonances of the alkyl side chains.^{68,69} Unexpectedly, we have achieved a significant enhancement in the molecular order, as evidenced by the GIWAXS experiments, with a slight decrease of the π -stacking

distance from 3.60 Å for the non-end-capped DTG–BTD to 3.55 Å for the end-capped analogue. As a result, end-capped DTG–BTD exhibited a maximum hole mobility of $0.60 \text{ cm}^2/(\text{Vs})$ —an order of increase relative to $0.077 \text{ cm}^2/(\text{Vs})$ for the non-end-capped polymer.

RESULTS AND DISCUSSION

The synthesis of end-capped (E) and non-end-capped (NE) DTG–BTD is outlined in **Scheme 1**, and details can be found in

the Supporting Information. The E(DTG–BTD) copolymer was prepared via a Kosugi–Migita–Stille polycondensation using a 1% stoichiometric excess of the distannylated monomer relative to the dibromo monomer, using $\text{Pd}_2(\text{dba})_3\text{:P}(o\text{-tol})_3$ as a catalyst for 3 days at 90 °C with the goal of optimizing the quantity of the end-capping sites as demonstrated previously.^{64,65} Tolyl end groups were incorporated at the end of the polymerization by addition of 4-iodotoluene and allowing the reaction to continue for a further 20 h. The NE polymer was prepared under identical polymerization conditions without the post-end-capping procedure. After the polymerizations, the reaction mixtures were precipitated into methanol, and the filtered polymers were washed via Soxhlet extraction using methanol, acetone, hexane, and chloroform. The chloroform soluble fractions were subsequently precipitated into methanol, affording the polymers in moderate yields of 68–70%. While the CHN elemental analyses of the polymers were obtained within the expected 0.4% theoretical limit (see Supporting Information), these results are not able to discern the possibility of small quantities of halogen end group or thieryl protons due to destannylation.

The polymers were fully soluble in tetrahydrofuran (THF) allowing GPC estimated molecular weights at 40 °C relative to the elution volume of polystyrene standards as shown in Figure S1. It is understood that these conjugated polymers are poorly represented by the random coil PS standards, but in the absence of more appropriate polyheterocycle-based standards, the relative comparison allows a first-order approximation. The overestimated GPC molecular weight values obtained by calibration with PS standards has been thoroughly analyzed for rigid-rod poly(*p*-phenylene) (PPP) type polymers by comparing results from the universal calibration based on Mark–Houwink–Sakurada equation and further by PPP standards. Also, as shown by molecular weight determinations for P3HT polymers comparing GPC, MALDI-MS, and H NMR results, it is concluded that in the medium range molecular weight regime (10–40 kDa) GPC overestimates the molecular weight by a factor of 1.3 or 1.7 reported by different groups.^{68,70–72} With this, E(DTG–BTD) had an estimated number-average molecular weight (M_n) of 33 kDa with a PDI of 2.43, while NE(DTG–BTD) exhibited a M_n of 28 kDa with a PDI of 2.66 with quite similar elution curve shapes. As a result, using THF as an eluent in the GPC experiments, we demonstrate that we have obtained polymers with elution volumes comparable to the elution volume of PS of molecular weight near 30 kDa allowing further comparison of their properties.

Detailed characterization of the end-group identity was carried out using ¹H NMR and MALDI-MS, in conjunction with XPS and ICP analyses to determine the level of success of the end-capping procedure. In particular, ¹H NMR and 2D NMR measurements were performed at 373 K in $\text{C}_2\text{D}_2\text{Cl}_4$ solvent, and the spectral differences of the polymers are highlighted in Figure 1.

First, the distinct chemical shift of the methyl protons on the tolyl moiety, ca. 2.3 ppm, is used to confirm the presence of tolyl end groups. As illustrated in Figure 1a, the presence of a peak at 2.38 ppm for E(DTG–BTD), which is absent in the spectrum of NE(DTG–BTD), identifies its presence as a chain end. To confirm this peak belongs to a tolyl moiety, 2D NMR experiments of ¹H, ¹³C HSQC and ¹H, ¹H NOESY were carried out. As seen in Figure 1b, the ¹H, ¹³C HSQC spectrum of E(DTG–BTD) shows a correlation pattern of the methyl proton peak with a carbon at 20.6 ppm as expected for a chemical shift of

a methyl carbon on tolyl. Further, ¹H, ¹H NOESY 2D experiments displayed a through-space correlation pattern of the peak at 2.38 ppm with aromatic protons at 7.22 ppm due to the phenylene protons on the tolyl moiety. In contrast, these correlation patterns were absent in the NE(DTG–BTD) polymer HSQC and NOESY spectra (Figures S2–S4). Additionally, comparison of the tolyl methyl proton integration with the peak corresponding to methyl protons on the *n*-dodecyl side chains allows estimation of the number-average degree of polymerization (X_n), with the assumption that the major fraction of chain ends have been capped. This ratio was found to be ca. 40 corresponding to a number-average molecular weight of 28 kDa, suggesting that the molecular weight found by GPC is slightly overestimated—a common observation in conjugated polymers.⁷³ Previous work by Muellen and co-workers has shown that variation between ¹H NMR and GPC values is due to the errors in signal integration in NMR due to broader polymer proton signals and also from the calibration standards used for GPC.⁷¹ It is worth noting here that ¹H NMR analyses do not elicit the extent of the end-capping on the polymer, whether both ends, one end, or none of the ends of the polymer chains are end-capped.

To probe this, we carried out matrix-assisted laser desorption–ionization (MALDI) mass spectrometry to examine the repeat units and the end groups on the polymers as seen in Figure S5. The mass spectra of both polymers exhibited oligomers ($n = 4–8$) separated by 708 amu, consistent with the calculated mass of the DTG–BTD repeat group. Figure 1e shows the expanded region of the mass spectrum in the range of m/z 2700 and m/z 3700 to study the nature of the end groups for the residual masses of oligomers present in E(DTG–BTD). Four major peaks, at m/z 2830, m/z 2880, m/z 2922, and m/z 2966, around the peak for $n = 4$ have been observed. The peak at m/z 2830 can be assigned to a tetramer having two hydrogen end groups, the peak at m/z 2880 to a trimer having two tolyl end groups, the peak at m/z 2922 is due to a tetramer with one tolyl and one hydrogen end group, and the peak at m/z 2966 is due to a tetramer with an additional BTD unit with two hydrogen end groups. Next, around the pentamer peak at m/z 3540 four other peaks are seen. The peak at m/z 3632 is due to a pentamer end-capped with a tolyl moiety and a hydrogen. The peaks at m/z 3404, m/z 3496, and m/z 3588 represent tetramers with an additional DTG unit (which is expected as the polymerization has been run for 1% in stoichiometric imbalance of the DTG ditin monomer) end-capped with hydrogens, a tolyl unit and a hydrogen, and two tolyl groups, respectively. In this regard, the chemistry shown in Figure S6 presents that hydrogen end groups are indicative of loss of the stannyll and bromine end-functionality during the course of polymerization possibly via competing side reactions of dehalogenation and destannylation which complicate the analysis of these results. Destannylation reactions have been considered because early studies of these coupling oligomerizations and polymerizations and similar observations were reported for Suzuki–Miyaura polycondensations.^{60,61} These side reactions render either dead polymer (oligomer) chains end-capped with hydrogen atoms or end-capping on the one end that still contains the reactive stannyll functional groups. Given that these side reactions are terminating the species probed most easily by MALDI-MS, it is suggested that the higher molecular weight materials likely have a more efficient end-capping.^{74,75} Using the Carothers equation as our basis, a 1% stoichiometric imbalance of the difunctional monomers and 98.5% extent of reaction should yield a number-average degree of

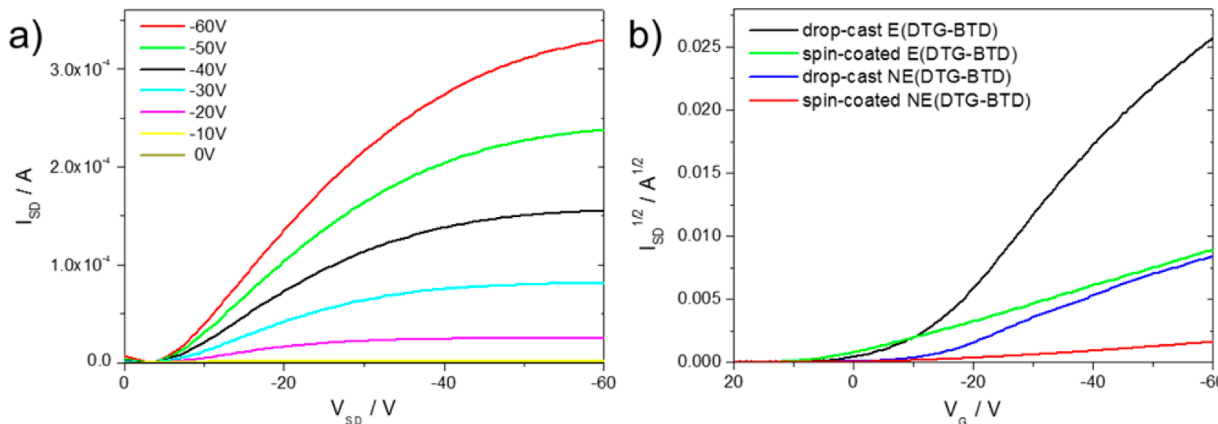


Figure 2. (a) Transistor output curves for drop-cast E(DTG–BTD) from a 2 mg/mL DCB solution onto hexamethylsilazane pretreated Si/SiO₂ bottom gate, bottom contact device substrates, and (b) transfer plots for all four polymer samples prepared by drop-casting and spin-coating.

polymerization (X_n) of 50 with no loss of polymerization functionality. We think that an extent of reaction less than unity is chosen by the observation of dead reactive chains resulting from the competing side reactions. Similarly, a strict relationship between monomer ratio and molecular weight was not observed by others, indicating an extent of reaction less than unity.⁴⁰ This problem was also recently discussed by You and co-workers, and they proposed strict purification of solid monomers via recrystallization multiple times and recrystallizing the Pd catalyst to remove the inactive Pd nanoparticles present and suggested a fast heating via microwave radiation.⁶⁶ Hence, the number-average degree of polymerization of 40 obtained by NMR is reasonable if most of the chains are end-capped with tolyl units.

X-ray photoelectron spectroscopy (XPS) was subsequently used to probe the absence or presence of Sn and Br atoms in an attempt to assess the success of the end-capping reactions as shown in Figure S7.⁵⁵ XPS spectra for the spin-coated films of E(DTG–BTD) and NE(DTG–BTD) using a Mg anode as the X-ray source detected the presence of Ge, N, C, and S in the composition of the repeat unit. No signals were obtained, indicating the expected Br 3d or Sn 3d_{5/2} signals as highlighted by blue and red arrows, respectively. Furthermore, an Al anode was employed as an X-ray source for XPS analysis of NE(DTG–BTD) to differentiate the sample's XPS peaks from Auger peaks, but no significant changes, except the disappearance of high-energy peaks due to Ge auger electrons, were observed. As the XPS spectra of the polymers did not yield substantial differences, we therefore conclude that while this method is a generally useful tool for determining elemental composition, it typically yields sensitivities within ~0.1% and is not capable of detecting the minimal content of Sn and Br in these polymers. Further, we carried out inductively coupled plasma (ICP) analyses to quantify the amount of Sn residues present in the polymers. The amount of Sn isotopes was found to be 1979 ppm (0.20 wt %) for E(DTG–BTD) and 1583 ppm (0.16 wt %) for NE(DTG–BTD), implying the Sn content is comparable in both polymers, and therefore we can speculate that residual tin atoms are either buried inside the polymer network or they are still bonded to DTG units unobservable within the ¹H NMR limits.

To probe the effect of end-capping on the charge carrier transport, OFET devices were prepared. The polymers were processed using two different conditions to determine that the device performance could be independent of processing parameters. The films were prepared by drop-casting from a 2

mg/mL dichlorobenzene (DCB) solution and by spin-coating a 10 mg/mL chloroform (CHCl₃) solution both onto hexamethylsilazane pretreated Si/SiO₂ bottom gate, bottom contact device substrates. Afterward, the samples were annealed at 200 °C for 60 min. The recorded OFET output plots are shown in Figure 2a and Figure S9 and confirm only holes as charge carriers for both polymers during device operation. The key performance values are summarized in Table 1 and indicate two major factors

Table 1. Overview of the Average OFET Charge Carrier Mobility and On/Off Ratio for E(DTG–BTD) and NE(DTG–BTD) Processed under Different Conditions

polymer	mobility/cm ² /(V s) (on/off ratio)	
	drop-cast DCB	spin-coated CHCl ₃
E(DTG–BTD)	$0.55 \pm 0.05 (9 \times 10^5)$	$0.043 \pm 0.013 (7 \times 10^4)$
NE(DTG–BTD)	$0.061 \pm 0.016 (2 \times 10^5)$	$0.002 \pm 0.0005 (1 \times 10^4)$

for the increase in mobility: (1) processing method (drop-casting vs spin-coating) and (2) chemical design by end-capping. Specifically, drop-casting resulted in films with higher hole mobilities compared to spin-coated films, while end-capped polymer showed higher mobility compared to the non-end-capped polymer in both processing methods. We attribute the rise in device performance in the drop-cast samples compared to spin-coated films to the crystallization kinetics during solvent evaporation. Since spin-coating is a rapid process, the final structural order is lower (see structural analysis below) due to insufficient crystallization time, leading to a kinetically trapped morphological state and relatively low charge mobility. Since solvent evaporation from the cast drop occurs over several minutes, slower solidification leads to higher crystallinity in the resulting film. At the same time, the difference in mobility we observe between E(DTG–BTD) and NE(DTG–BTD) using the same deposition conditions is clear evidence for an important role of end-capping on the charge carrier mobility. Given the complexity of the end-capping chemistry discussed above, we ask the question: how do the end groups affect polymer organization? As charge transport is directly related to the structural order, we next investigated the molecular organization and microstructure of the bulk films in an attempt to understand this dramatic variation in transport performance between the polymers caused by the end groups.

The grazing incidence wide-angle X-ray scattering (GIWAXS) patterns from films prepared via both drop-casting and spin-

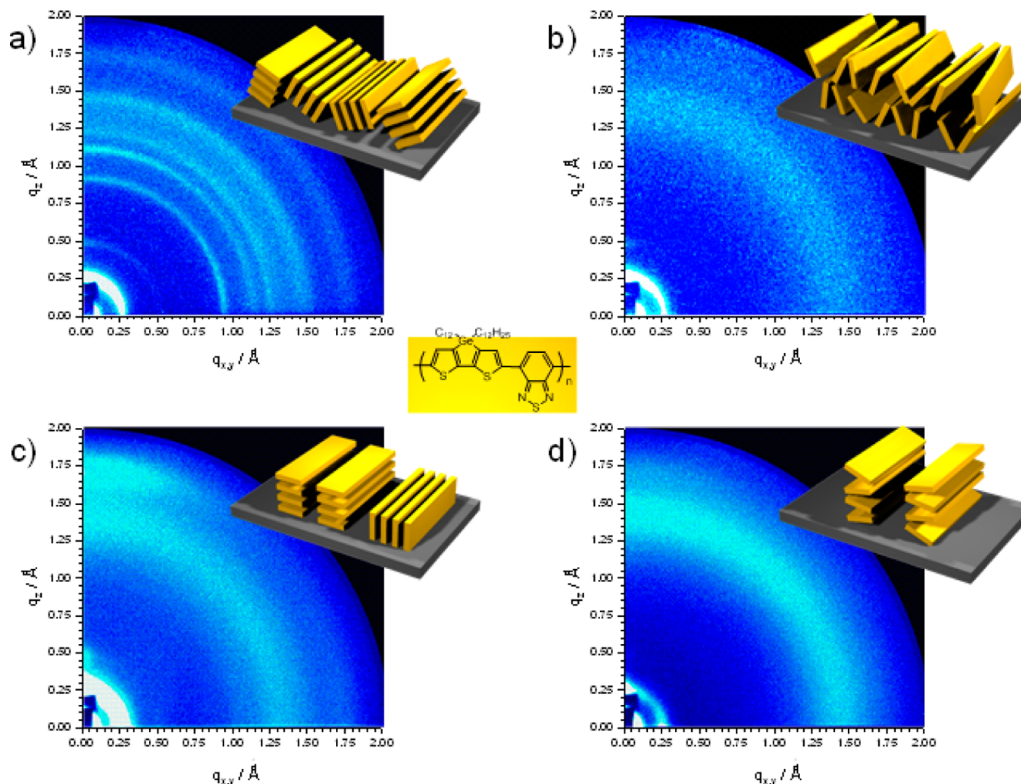


Figure 3. GIWAXS patterns of drop-cast (a) and spin-coated (c) of E(DTG-BTD), along with drop-cast (b) and spin-coated (d) of NE(DTG-BTD). Insets schematically illustrate the surface organization of the polymers (yellow boards represent polymer backbones; for sake of simplicity side chains and dispersity are not taken into account): (a) disordered crystallites, (b) intralamellar disorder, (c) face-on with minor edge-on arrangement, and (d) disordered face-on organization.

coating display significant variations in order between E(DTG-BTD) and NE(DTG-BTD). A high number of relative isotropic reflections appear in the pattern of Figure 3a for drop-cast E(DTG-BTD), indicating ordered polymer backbones in lamellar structures but random orientation of domains with respect to each other and the surface.^{76,77} This lack of polymer chain long-range alignment is attributed to the drop-casting of the solution and the random nucleation and self-assembly during solvent evaporation. The schematic organization of the polymer chains is illustrated in the inset of Figure 3a. The meridional integration along q_z at $q_{x,y} = 0 \text{ \AA}^{-1}$ in Figure 4a allows the derivation of a π -stacking distance of 3.55 Å for E(DTG-BTD). In stark contrast to this organization, NE(DTG-BTD) reveals no reflections in the middle- and wide-angle area (large q values), which is characteristic for low interchain order resulting from poor interactions between conjugated backbones (Figure 3b). Only a typical amorphous halo is present in the meridional integration of the pattern in Figure 4a which is related to the flexible alkyl side chains. The polymer chains of NE(DTG-BTD) form lamellar stacks as confirmed by the small-angle scattering intensities, in which, however, the backbones are highly disordered (see schematic illustration in inset of Figure 3b). We attribute the drastic drop in mobility for the drop-cast films, from $0.6 \text{ cm}^2/(\text{V s})$ for E(DTG-BTD) to $0.077 \text{ cm}^2/(\text{V s})$ for NE(DTG-BTD) to this decrease in order. The aforementioned trend is maintained for the spin-coated layers, although the magnitude of the charge mobilities is lower. The pronounced meridional ($q_{x,y} = 0 \text{ \AA}^{-1}$) wide-angle reflection in the GIWAXS pattern shown in Figure 3c for E(DTG-BTD) corresponds to the π -stacking distance of 3.55 Å of preferentially face-on arranged polymer backbones on the surface. Additional

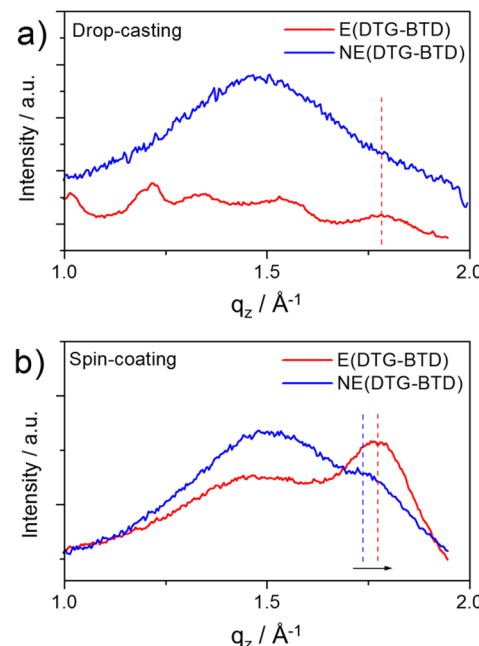


Figure 4. GIWAXS integrations of the wide-angle scattering region along q_z at $q_{x,y} = 0 \text{ \AA}^{-1}$ for E(DTG-BTD) and NE(DTG-BTD) after (a) drop-casting and (b) spin-coating. The dashed lines mark the position of the π -stacking peak maximum for E(DTG-BTD) (red) and NE(DTG-BTD) (blue). The arrow in (b) indicates the shift of the π -stacking distance from 3.60 Å for NE(DTG-BTD) to 3.55 Å for E(DTG-BTD).

weak scattering intensities in the equatorial plane of the pattern and the same q position suggest that a minor fraction of the polymers also organize edge-on. Such hybrid polymer arrangement might be due to stronger aggregation in solution⁵ as mediated by the presence of end-capping groups and has been discussed in terms of device improvement via 3D charge carrier transport in polymer thin film transistors.⁶ It is expected that the face-on arrangement favors the charge carrier transport perpendicular to the surface opening the possibility of bypassing structural defects more efficiently in comparison to a pure edge-on organization. The polymer spin-coated film of NE(DTG–BTD) also arranges face-on as implied by the meridional reflection (Figure 3d); however, the polymer ordering is significantly lower in comparison to spin-coated E(DTG–BTD). First, for NE(DTG–BTD) the intensity of the meridional reflection is decreased, while at the same time the amorphous halo increased. Second, the peak broadens, which is characteristic of a reduction in the ordered crystalline packing (Figure 4b). These enlarged crystallites for E(DTG–BTD) along the packing direction can be attributed to the introduction of the tolyl end-capping groups. Structural differences are also obvious from UV-vis absorption measurements in solution and in thin film indicating large variations in interactions between both polymers. Figure 1f shows the absorption spectra of the polymers in dilute toluene solutions and thin films. In solution, NE(DTG–BTD) demonstrates dual band absorption maxima at 420 and 684 nm, with a trough at 482 nm. This is similar to the solution spectrum obtained for of E(DTG–BTD) which, however, possesses an additional shoulder around 800 nm (see dotted arrow), suggesting some aggregation in the solvent. In thin film, both polymers preserve their aforementioned dual band absorption profiles. For E(DTG–BTD) there is a 15 nm red-shift in the low-energy band maximum, as well as a shoulder around 775 nm, which is more pronounced in the thin film spectrum than it was previously in the solution spectrum. This red-shifted shoulder is attributed to a vibronic aggregation band indicative of more ordered planar chains.^{3,7,8}

In addition to the X-ray evident interchain interactions, the microstructure is another essential issue for macroscopic charge carrier transport in organic electronic devices. The microstructure includes factors such as domain size and relative domain arrangement at grain boundaries. A small average size of the domains and thus higher density of domain boundaries might hamper charge carrier transport. Atomic force microscopy (AFM) was used to gain information about the film's surface topography. Interestingly, as presented in Figure 5a,b, drop-cast E(DTG–BTD) and NE(DTG–BTD) exhibit a similar type of network-like microstructure. However, in the case of E(DTG–BTD) this network is denser and finer, while the microstructure of NE(DTG–BTD) shows larger feature sizes. It can be assumed that a denser network provides more possible pathways for charge carriers in comparison to a more open meshed layer. The spin-coated samples also exhibit differences of the surface microstructure. While the E(DTG–BTD) layer consists of fine, short interconnected fibers, NE(DTG–BTD) reveals a globular topography of small spheres which are distributed over the top surface of the film (Figure 5c,d). The type of microstructure for each processing method can be explained in terms of the influence of tolyl end-capping groups on different molecular interactions of E(DTG–BTD) and NE(DTG–BTD). The improved π -stacking forces between E(DTG–BTD) polymer chains lead to the self-assembly into ordered, interconnected fibrous microstructure, while the reduced interactions in

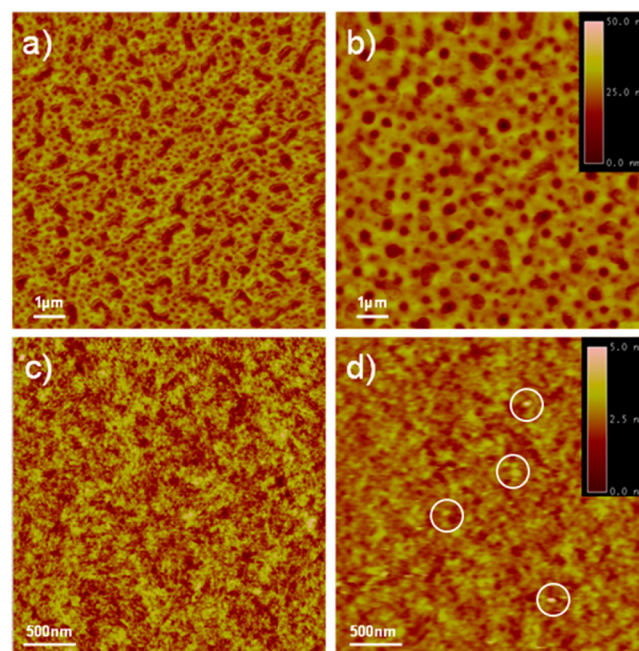


Figure 5. Tapping mode AFM height images of drop-cast and spin-coated (a, c) E(DTG–BTD) along with drop-cast and spin-coated (b, d) NE(DTG–BTD) (white circles indicate representative small spherical aggregates). Height scale is identical for each image.

NE(DTG–BTD) result in isotropic, single objects which might impede the charge carriers at the boundaries of these globular entities.

CONCLUSIONS

Considering OFET applications, the charge transport properties of conjugated polymers can be enhanced through a combination of both chemical design and morphological modifications induced via solution processing techniques. In this work, we have probed how polymer chain end-capping can be used to introduce tolyl end groups on a fraction of the polymer chains in a DTG–BTD donor–acceptor polymer system. We note that the charge transport properties of the end-capped DTG–BTD polymers are superior to the properties of its non-end-capped analogue, with the transistor mobility increased by ca. 1 order of magnitude for the end-capped polymer. We attribute these results to enhanced interchain interactions which induce dramatic improvements of the polymer organization in thin films, as evidenced by GIWAXS analyses. The question remains: why do we observe such a major structural order and transport effect induced by relatively small changes brought by the incorporation of a fraction of end groups on these conjugated polymers? We speculate that the tolyl end groups assist in aggregate formation (observed spectroscopically in both the processing solutions and solid films), increasing the polymer ordering and connectivity between crystallites. This enables more pathways for charge percolation leading to high charge carrier mobilities. As molecular order is an especially important parameter for high mobility, we believe this approach holds great promise in designing future polymers with high charge carrier mobilities. End-capping during the formation of polymers via Stille, Suzuki, direct arylation, and other metal-mediated coupling processes has become a common part of the polymer isolation process. At the same time, little is known about the efficacy of these reactions (as we have probed with the

combination of MALDI-MS and H NMR analyses). Based on these conclusions, various important questions arise. First, one wonders how many previous polymers whose transport and photovoltaic properties have been reported might have enhanced properties with proper end-capping? Second, one asks how polymerization scientists can most effectively carry out these end-capping reactions, and how can the end-capped structures be fully and properly characterized? Certainly, this is food for thought.

■ ASSOCIATED CONTENT

Supporting Information

The Supporting Information is available free of charge on the ACS Publications website at DOI: [10.1021/acs.macromol.5b01252](https://doi.org/10.1021/acs.macromol.5b01252).

Materials and methods, polymer synthesis, ¹H NMR, 2D NMR spectra, differential pulse voltammetry plots, MALDI-MS, XPS, ultraviolet–visible absorption spectra, OFET output and transfer plots ([PDF](#))

■ AUTHOR INFORMATION

Corresponding Authors

*(K.M.) E-mail: muellen@mpip-mainz.mpg.de.

*(W.P.) E-mail: pisula@mpip-mainz.mpg.de.

*(J.R.R.) E-mail: Reynolds@chemistry.gatech.edu.

Notes

The authors declare no competing financial interest.

■ ACKNOWLEDGMENTS

The authors thank the German Science Foundation (Korean-German IRTG). J.R.R. acknowledges the AFOSR (FA9550-09-1-0320) for the DTG–BTD syntheses. The authors thank Dr. Adam Kiersnowski for helpful discussions and technical support for GIWAXS.

■ REFERENCES

- (1) Kim, D. H.; Park, Y. D.; Jang, Y.; Yang, H.; Kim, Y. H.; Han, J. I.; Moon, D. G.; Park, S.; Chang, T.; Chang, C.; Joo, M.; Ryu, C. Y.; Cho, K. *Adv. Funct. Mater.* **2005**, *15* (1), 77–82.
- (2) Sirringhaus, H.; Tessler, N.; Friend, R. H. *Science* **1998**, *280* (5370), 1741–1744.
- (3) Lee, M. J.; Gupta, D.; Zhao, N.; Heeney, M.; McCulloch, I.; Sirringhaus, H. *Adv. Funct. Mater.* **2011**, *21* (5), 932–940.
- (4) McCulloch, I.; Heeney, M.; Bailey, C.; Genevicius, K.; MacDonald, I.; Shkunov, M.; Sparrowe, D.; Tierney, S.; Wagner, R.; Zhang, W.; Chabinyc, M. L.; Kline, R. J.; McGehee, M. D.; Toney, M. F. *Nat. Mater.* **2006**, *5* (4), 328–333.
- (5) Chen, M. S.; Lee, O. P.; Niskala, J. R.; Yiu, A. T.; Tassone, C. J.; Schmidt, K.; Beaujuge, P. M.; Onishi, S. S.; Toney, M. F.; Zettl, A.; Fréchet, J. M. J. *J. Am. Chem. Soc.* **2013**, *135* (51), 19229–19236.
- (6) Mei, J.; Kim, D. H.; Ayzner, A. L.; Toney, M. F.; Bao, Z. *J. Am. Chem. Soc.* **2011**, *133* (50), 20130–20133.
- (7) Guo, X.; Ortiz, R. P.; Zheng, Y.; Kim, M.-G.; Zhang, S.; Hu, Y.; Lu, G.; Facchetti, A.; Marks, T. J. *J. Am. Chem. Soc.* **2011**, *133* (34), 13685–13697.
- (8) Li, Y.; Singh, S. P.; Sonar, P. *Adv. Mater.* **2010**, *22* (43), 4862–4866.
- (9) Guo, X.; Kim, F. S.; Jenekhe, S. A.; Watson, M. D. *J. Am. Chem. Soc.* **2009**, *131* (21), 7206–7207.
- (10) Osaka, I.; Zhang, R.; Liu, J.; Smilgies, D.-M.; Kowalewski, T.; McCullough, R. D. *Chem. Mater.* **2010**, *22* (14), 4191–4196.
- (11) Zhang, M.; Tsao, H. N.; Pisula, W.; Yang, C.; Mishra, A. K.; Müllen, K. *J. Am. Chem. Soc.* **2007**, *129* (12), 3472–3473.
- (12) Zhang, F.; Hu, Y.; Schuettfort, T.; Di, C.-A.; Gao, X.; McNeill, C. R.; Thomsen, L.; Mannsfeld, S. C. B.; Yuan, W.; Sirringhaus, H.; Zhu, D. *J. Am. Chem. Soc.* **2013**, *135* (6), 2338–2349.
- (13) Mei, J.; Diao, Y.; Appleton, A. L.; Fang, L.; Bao, Z. *J. Am. Chem. Soc.* **2013**, *135* (18), 6724–6746.
- (14) Lei, T.; Dou, J.-H.; Cao, X.-Y.; Wang, J.-Y.; Pei, J. *J. Am. Chem. Soc.* **2013**, *135* (33), 12168–12171.
- (15) Lee, J.; Han, A. R.; Yu, H.; Shin, T. J.; Yang, C.; Oh, J. H. *J. Am. Chem. Soc.* **2013**, *135* (25), 9540–9547.
- (16) Kang, I.; Yun, H.-J.; Chung, D. S.; Kwon, S.-K.; Kim, Y.-H. *J. Am. Chem. Soc.* **2013**, *135* (40), 14896–14899.
- (17) Kaake, L. G.; Barbara, P. F.; Zhu, X. Y. *J. Phys. Chem. Lett.* **2010**, *1* (3), 628–635.
- (18) Lei, T.; Wang, J.-Y.; Pei, J. *Acc. Chem. Res.* **2014**, *47* (4), 1117–1126.
- (19) Tsao, H. N.; Cho, D.; Andreasen, J. W.; Rouhanipour, A.; Breiby, D. W.; Pisula, W.; Müllen, K. *Adv. Mater.* **2009**, *21* (2), 209–212.
- (20) Becerril, H. A.; Roberts, M. E.; Liu, Z.; Locklin, J.; Bao, Z. *Adv. Mater.* **2008**, *20* (13), 2588–2594.
- (21) Facchetti, A. *Chem. Mater.* **2011**, *23* (3), 733–758.
- (22) Usta, H.; Facchetti, A.; Marks, T. J. *Acc. Chem. Res.* **2011**, *44* (7), 501–510.
- (23) Wang, C.; Dong, H.; Hu, W.; Liu, Y.; Zhu, D. *Chem. Rev.* **2012**, *112* (4), 2208–2267.
- (24) Noriega, R.; Rivnay, J.; Vandewal, K.; Koch, F. P. V.; Stingelin, N.; Smith, P.; Toney, M. F.; Salleo, A. *Nat. Mater.* **2013**, *12* (11), 1038–1044.
- (25) Ho, V.; Boudouris, B. W.; Segalman, R. A. *Macromolecules* **2010**, *43* (19), 7895–7899.
- (26) Beaujuge, P. M.; Tsao, H. N.; Hansen, M. R.; Amb, C. M.; Risko, C.; Subbiah, J.; Choudhury, K. R.; Mavrinckiy, A.; Pisula, W.; Brédas, J.-L.; So, F.; Müllen, K.; Reynolds, J. R. *J. Am. Chem. Soc.* **2012**, *134* (21), 8944–8957.
- (27) Garnier, F.; Yassar, A.; Hajlaoui, R.; Horowitz, G.; Deloffre, F.; Servet, B.; Ries, S.; Alnot, P. *J. Am. Chem. Soc.* **1993**, *115* (19), 8716–8721.
- (28) Lee, J. S.; Son, S. K.; Song, S.; Kim, H.; Lee, D. R.; Kim, K.; Ko, M. J.; Choi, D. H.; Kim, B.; Cho, J. H. *Chem. Mater.* **2012**, *24* (7), 1316–1323.
- (29) Lei, T.; Dou, J.-H.; Pei, J. *Adv. Mater.* **2012**, *24* (48), 6457–6461.
- (30) Kim, Y.; Cook, S.; Tuladhar, S. M.; Choulis, S. A.; Nelson, J.; Durrant, J. R.; Bradley, D. D. C.; Giles, M.; McCulloch, I.; Ha, C.-S.; Ree, M. *Nat. Mater.* **2006**, *5* (3), 197–203.
- (31) Ong, B. S.; Wu, Y.; Liu, P.; Gardner, S. *J. Am. Chem. Soc.* **2004**, *126* (11), 3378–3379.
- (32) Zen, A.; Pflaum, J.; Hirschmann, S.; Zhuang, W.; Jaiser, F.; Asawapirom, U.; Rabe, J. P.; Scherf, U.; Neher, D. *Adv. Funct. Mater.* **2004**, *14* (8), 757–764.
- (33) Kline, R. J.; McGehee, M. D.; Kadnikova, E. N.; Liu, J.; Fréchet, J. M. *J. Adv. Mater.* **2003**, *15* (18), 1519–1522.
- (34) Tsao, H. N.; Cho, D. M.; Park, I.; Hansen, M. R.; Mavrinckiy, A.; Yoon, D. Y.; Graf, R.; Pisula, W.; Spiess, H. W.; Müllen, K. *J. Am. Chem. Soc.* **2011**, *133* (8), 2605–2612.
- (35) Donley, C. L.; Zaumseil, J.; Andreasen, J. W.; Nielsen, M. M.; Sirringhaus, H.; Friend, R. H.; Kim, J.-S. *J. Am. Chem. Soc.* **2005**, *127* (37), 12890–12899.
- (36) Rieger, R.; Beckmann, D.; Pisula, W.; Steffen, W.; Kastler, M.; Müllen, K. *Adv. Mater.* **2010**, *22* (1), 83–86.
- (37) Lei, T.; Cao, Y.; Zhou, X.; Peng, Y.; Bian, J.; Pei, J. *Chem. Mater.* **2012**, *24* (10), 1762–1770.
- (38) Osaka, I.; Abe, T.; Shinamura, S.; Takimiya, K. *J. Am. Chem. Soc.* **2011**, *133* (17), 6852–6860.
- (39) Kim, S.; Park, J. K.; Park, Y. D. *RSC Adv.* **2014**, *4* (74), 39268–39272.
- (40) Gibson, G. L.; Gao, D.; Jahnke, A. A.; Sun, J.; Tilley, A. J.; Seferos, D. S. *J. Mater. Chem. A* **2014**, *2* (35), 14468–14480.
- (41) McCullough, R. D.; Lowe, R. D.; Jayaraman, M.; Anderson, D. L. *J. Org. Chem.* **1993**, *58* (4), 904–912.

- (42) McCullough, R. D.; Tristram-Nagle, S.; Williams, S. P.; Lowe, R. D.; Jayaraman, M. *J. Am. Chem. Soc.* **1993**, *115* (11), 4910–4911.
- (43) Loewe, R. S.; Khersonsky, S. M.; McCullough, R. D. *Adv. Mater.* **1999**, *11* (3), 250–253.
- (44) Loewe, R. S.; Ewbank, P. C.; Liu, J.; Zhai, L.; McCullough, R. D. *Macromolecules* **2001**, *34* (13), 4324–4333.
- (45) Krüger, R. A.; Gordon, T. J.; Baumgartner, T.; Sutherland, T. C. *ACS Appl. Mater. Interfaces* **2011**, *3* (6), 2031–2041.
- (46) Boudouris, B. W.; Molins, F.; Blank, D. A.; Frisbie, C. D.; Hillmyer, M. A. *Macromolecules* **2009**, *42* (12), 4118–4126.
- (47) Moon, H. C.; Anthonysamy, A.; Lee, Y.; Kim, J. K. *Macromolecules* **2010**, *43* (4), 1747–1752.
- (48) Chen, Y.-H.; Huang, P.-T.; Lin, K.-C.; Huang, Y.-J.; Chen, C.-T. *Org. Electron.* **2012**, *13* (2), 283–289.
- (49) Lohwasser, R. H.; Thelakkat, M. *Macromolecules* **2010**, *43* (18), 7611–7616.
- (50) Lohwasser, R. H.; Bandara, J.; Thelakkat, M. *J. Mater. Chem.* **2009**, *19* (24), 4126–4130.
- (51) Jeffries-El, M.; Sauvé, G.; McCullough, R. D. *Macromolecules* **2005**, *38* (25), 10346–10352.
- (52) Kochemba, W. M.; Pickel, D. L.; Sumpter, B. G.; Chen, J.; Kilbey, S. M. *Chem. Mater.* **2012**, *24* (22), 4459–4467.
- (53) Zou, Y.; Najari, A.; Berrouard, P.; Beaupré, S.; Réda Aïch, B.; Tao, Y.; Leclerc, M. *J. Am. Chem. Soc.* **2010**, *132* (15), 5330–5331.
- (54) InganÅs, O.; Zhang, F.; Andersson, M. R. *Acc. Chem. Res.* **2009**, *42* (11), 1731–1739.
- (55) Park, J. K.; Jo, J.; Seo, J. H.; Moon, J. S.; Park, Y. D.; Lee, K.; Heeger, A. J.; Bazan, G. C. *Adv. Mater.* **2011**, *23* (21), 2430–2435.
- (56) Rudenko, A. E.; Thompson, B. C. *J. Polym. Sci., Part A: Polym. Chem.* **2015**, *53* (2), 135–147.
- (57) Wakioka, M.; Ichihara, N.; Kitano, Y.; Ozawa, F. *Macromolecules* **2014**, *47* (2), 626–631.
- (58) Asaoka, S.; Takeda, N.; Iyoda, T.; Cook, A. R.; Miller, J. R. *J. Am. Chem. Soc.* **2008**, *130* (36), 11912–11920.
- (59) Shim, C.; Kim, M.; Ihn, S.-G.; Choi, Y. S.; Kim, Y.; Cho, K. *Chem. Commun.* **2012**, *48* (57), 7206–7208.
- (60) Groenendaal, L.; Peerlings, H. W. I.; Havinga, E. E.; Vekemans, J. A. J. M.; Meijer, E. W. *Synth. Met.* **1995**, *69* (1–3), 467–470.
- (61) Jayakannan, M.; van Dongen, J. L. J.; Janssen, R. A. J. *Macromolecules* **2001**, *34* (16), 5386–5393.
- (62) Baycan Koyuncu, F.; Davis, A. R.; Carter, K. R. *Chem. Mater.* **2012**, *24* (22), 4410–4416.
- (63) Robb, M. J.; Montarnal, D.; Eisenmenger, N. D.; Ku, S.-Y.; Chabiny, M. L.; Hawker, C. J. *Macromolecules* **2013**, *46* (16), 6431–6438.
- (64) Huang, H.; Cao, Z.; Gu, Z.; Li, X.; Zhao, B.; Shen, P.; Tan, S. *Eur. Polym. J.* **2012**, *48* (10), 1805–1813.
- (65) Cox, J. R.; Kang, H. A.; Igarashi, T.; Swager, T. M. *ACS Macro Lett.* **2012**, *1* (2), 334–337.
- (66) Li, W.; Yang, L.; Tumbleston, J. R.; Yan, L.; Ade, H.; You, W. *Adv. Mater.* **2014**, *26* (26), 4456–4462.
- (67) Amb, C. M.; Chen, S.; Graham, K. R.; Subbiah, J.; Small, C. E.; So, F.; Reynolds, J. R. *J. Am. Chem. Soc.* **2011**, *133* (26), 10062–10065.
- (68) Wong, M.; Hollinger, J.; Kozycz, L. M.; McCormick, T. M.; Lu, Y.; Burns, D. C.; Seferos, D. S. *ACS Macro Lett.* **2012**, *1* (11), 1266–1269.
- (69) Okamoto, K.; Luscombe, C. K. *Chem. Commun.* **2014**, *50* (40), 5310–5312.
- (70) Vanhee, S.; Rulkens, R.; Lehmann, U.; Rosenauer, C.; Schulze, M.; Köhler, W.; Wegner, G. *Macromolecules* **1996**, *29* (15), 5136–5142.
- (71) Francke, V.; Mangel, T.; Müllen, K. *Macromolecules* **1998**, *31* (8), 2447–2453.
- (72) Zhang, R.; Li, B.; Iovu, M. C.; Jeffries-El, M.; Sauvé, G.; Cooper, J.; Jia, S.; Tristram-Nagle, S.; Smilgies, D. M.; Lambeth, D. N.; McCullough, R. D.; Kowalewski, T. *J. Am. Chem. Soc.* **2006**, *128* (11), 3480–3481.
- (73) Hohl, B.; Bertschi, L.; Zhang, X.; Schlüter, A. D.; Sakamoto, J. *Macromolecules* **2012**, *45* (13), 5418–5426.
- (74) Schriemer, D. C.; Li, L. *Anal. Chem.* **1997**, *69* (20), 4169–4175.
- (75) Schriemer, D. C.; Li, L. *Anal. Chem.* **1997**, *69* (20), 4176–4183.
- (76) Fuoss, P. H.; Brennan, S. *Annu. Rev. Mater. Sci.* **1990**, *20* (1), 365–390.
- (77) DeLongchamp, D. M.; Kline, R. J.; Fischer, D. A.; Richter, L. J.; Toney, M. F. *Adv. Mater.* **2011**, *23* (3), 319–337.
- (78) Mortimer, R. J.; Graham, K. R.; Grenier, C. R. G.; Reynolds, J. R. *ACS Appl. Mater. Interfaces* **2009**, *1* (10), 2269–2276.